Capacity drops at merges

Analytical expressions for multilane freeways

Leclercq, L.; Knoop, Victor; Marczak, F; Hoogendoorn, Serge

Important note
To cite this publication, please use the final published version (if applicable).
Please check the document version above.

Capacity Drops at Merges
Analytical Expressions for Multilane Freeways

Ludovic Leclercq, Florian Marczak, Victor L. Knoop,
and Serge P. Hoogendoorn

This paper deals with the derivation of analytical formulas to estimate the effective capacity at freeway merges in a multilane context. The paper extends the findings presented in two previous papers describing studies that were based on the same modeling framework but that were restricted to a single lane on the freeway (or to the analysis of the right lane only). The analytical expression for the one-lane capacity was recursively applied to all lanes. Lane-changing maneuvers (mandatory for the on-ramp vehicles and discretionary for the other vehicles) were divided into two nonoverlapping local merging areas. Discretionary lane changes were transformed into a lane-changing flow by the use of appropriate analytical formulas. These formulas defined a system of equations whose unknowns were the capacity on all lanes and the inserting flow coming from the on-ramp. A sensitivity analysis showed that vehicle acceleration and the truck ratio were the parameters that most influenced the total capacity. The results obtained with the analytical formulas were proven to match the numerical results obtained from a traffic simulator that fully describes vehicle dynamics. Finally, the results provide good estimates in comparison with experimental data for an active merge on the M6 Motorway in the United Kingdom.

Two key figures that are used to describe merges on freeways are the merge ratio and the effective capacity. The merge ratio represents how the incoming flows share the downstream effective capacity in congestion (*1–3*). Experimental evidence from many different locations demonstrates that this ratio is fixed whatever the downstream flow value is (*3–6*). The effective capacity corresponds to the maximum flow that can be observed downstream of congested merges. It is observed when downstream traffic conditions are in free flow and so the merge acts as an active bottleneck. Effective capacity is also referred to in some papers, for example, as the queue discharge rate because the congestion head is located close to the merge (*7, 8*).

Experimental findings show that the effective capacity is classically below the maximal observed flow in free flow by a magnitude of between 10% and 30% (*8–15*; Zheng et al., unpublished work). Several physical explanations of such a capacity drop have been proposed in the literature: merging vehicles insert at lower

L. Leclercq, Université de Lyon, Institut Français des Sciences et Technologies du Transport du l'Aménagement et des Réseaux, Ecole Nationale des Travaux Publics de l'Etat, Laboratoire Ingénierie Circulation Transport, Rue Maurice Audin, F-69518 Lyon, France. F. Marczak, Direction Régionale de l'Environnement, de l'Aménagement et du Logement–Alsace, BP 81005, F-67070 Strasbourg, France. V. L. Knoop and S. P. Hoogendoorn, Delft University of Technology, Stevinweg 1, Delft, Netherlands. Corresponding author: L. Leclercq, ludovic.leclercq@entpe.fr.

speeds and need time to accelerate (*16–19*), the impacts of different driver behaviors or car characteristics (*5, 7, 20, 21*), and lane changes and the global acceleration process that happens downstream of the merge (*22, 23*). Most of these explanations involve the acceleration patterns of slower vehicles that create in front of them local voids that temporarily reduce the flow.

Except for direct experimental observations, the most common way to determine the effective merge capacity is to use a traffic model able to reproduce the underlying physical mechanisms (*15–19*; Zheng et al., unpublished work). Use of such a traffic model requires a simulation to be run for every new set of parameters and is not convenient when one is looking for a first and quick approximation of how a merge behaves. To the authors' knowledge, Leclercq et al. were the first to propose a different approach based on analytical considerations (*24*). The main source of the capacity drop is supposed to be the inserting vehicles. These vehicles are considered to act as moving bottlenecks with a bounded acceleration (*25, 26*), whereas mainstream vehicles are reproduced by the kinematic wave theory with a triangular fundamental diagram (*27, 28*).

Leclercq et al. provided an implicit analytical expression that defines the effective capacity of a congested merge with respect to the fundamental diagram parameters, the value of acceleration, the merge ratio, and the length of the on-ramp (*24*). This first attempt had three main shortcomings. First, the application of the kinematic wave theory was oversimplified and did not consider the interactions between the downstream congestion waves and voids that appear in front of inserting vehicles (moving bottlenecks). Second, vehicle characteristics and, in particular, their acceleration rate and size (jam density) were considered homogeneous. Third, the analytical derivations were provided only for a one-lane freeway. Extensions to multilane cases have been discussed, but the authors were able to define only a simple method that provides large bounds and not a direct value for the total effective capacity (*24*).

Recently, new analytical investigations in line with the previous framework have been proposed (*29*). These new methods allow the first two shortcomings to be eliminated. First, the interactions between waves and voids are properly handled and integrated in a refined implicit analytical expression. It appears that the capacity value increases by 15% to 20% when such interactions are considered for the same parameter settings. The capacity value is increased because waves are delayed by voids, which increase the available capacity. Second, characteristics of heterogeneous vehicles were introduced. The acceleration rate for the insertion of vehicles and the jam density can then be distributed to distinguish the effects of cars and trucks. The main conclusion for this second extension is

that consideration of the distribution of these parameters has little impact on the mean effective capacity, as long as the mean value for each parameter is properly estimated.

The study described here focused entirely on the last shortcoming, that is, the multilane extension. This focus implies that not only mandatory lane changes that correspond to inserting vehicles but also discretionary lane changes that correspond to vehicles that want to avoid the inserting area must be considered. A global framework is proposed to determine the effective capacity for all freeway lanes while accounting for both of these phenomena. This framework leads to an implicit and well-defined system of equations whose solutions provide the local capacity on all lanes and the inserting flow when the merge is an active bottleneck. The results obtained with the global analytical model were compared with outputs from a classical traffic simulator and experimental data to demonstrate its performance.

This paper is organized as follow: the next section presents the global modeling framework. The subsequent section focuses on numerical investigations with both a sensitivity analysis and a comparison with simulation outputs. A first experimental validation of the model at the same experimental site used in a previous study is then provided (24). The findings notably show that the new framework leads to analytical estimates that are close to observations, whereas the original frameworks provided only large bounds. A brief conclusion is then presented.

MODELING FRAMEWORK

This section presents the modeling framework for a two-lane freeway. Extension to higher lane numbers can be obtained in a recursive manner, as presented below for a three-lane freeway.

Partitioning of a Multilane Merge in Different Local Merges

A complete description of the physical mechanisms that can be observed at a congested freeway merge was derived from experimental observations (16). First, inserting vehicles that realize mandatory lane changes tend to reduce the average speed in the right lane when they become too numerous (see Area 1 in Figure 1a). This situation is the primary cause for the capacity drop. Vehicles from the freeway then try to avoid the speed reduction in the right lane by moving to the left lane (see Area 2 in Figure 1a). Such discretionary lane changes start happening at lower speeds when the congestion is well established in the right lane. Thus, the capacity reduction spreads over the other lane because of the lane-changing

process. In the end, all lanes experience congested traffic states and the exit flow from the bottleneck corresponds to the effective capacity. Discretionary lane changes can also be observed downstream of the inserting area, but they do not really influence the capacity value because they happen at higher speeds (see Area 3 in Figure 1a).

To derive an analytical formulation of the effective capacity of a multilane merge, the physical process must be simplified. In particular, the different lane-changing maneuvers need to be partitioned into several nonoverlapping spatial areas. Otherwise, it would be too difficult to resort analytically to the conservation principle for each lane because lateral flows would be observed in both lanes. Such a spatial partitioning is consistent with the physical mechanisms described elsewhere (16). Here it is assumed that the discretionary lane changes from Lane 1 to Lane 2 happen first in an area located just upstream of the on-ramp, that is, the blue area in Figure 1b. The length of the discretionary lane-changing area is denoted L_{DLC}. The mandatory lane changes from the on-ramp to Lane 1 and then happens in the red area in Figure 1b. The length of the inserting area is L. Both areas (blue and red) are consecutive with no overlap. They define a spatial partition corresponding to two consecutive merges, that is, Merges 2 and 1 in Figure 1b. When all lanes are congested, the exit flows from Lanes 1 and 2 are equal to their respective effective capacities, C_1 and C_2. Let q_0 and q_{12} denote the inserting flows for Merges 1 and 2, respectively, and let q_1 and q_2 denote the main inflows for Merges 1 and 2, respectively (Figure 1b). The result is

$$\begin{cases} q_0 + q_1 = C_1 & \text{(Merge 1)} \\ q_{12} + q_2 = C_2 & \text{(Merge 2)} \end{cases} \tag{1}$$

This formal representation neglects the discretionary lane changing that can be observed downstream of the on-ramp (see Area 3 in Figure 1a). As mentioned above, such lane changes are not numerous compared with the numbers of lane changes that occur in Areas 1 and 2. Furthermore, their contribution to the capacity drop is low because most of the flow obstructions appear upstream of the on-ramp. This finding means that lane changes in Area 3 benefit from voids created upstream. Therefore, the authors claim that this hypothesis has limited impacts on the calculation of the effective capacity for all lanes. This claim is supported by the results of the experimental investigations presented below.

Finally, Merge 1 corresponds to the usual merging process that can be represented by the well-known Daganzo merge model (2). Let α_l denote the local merge ratio between the on-ramp and Lane 1.

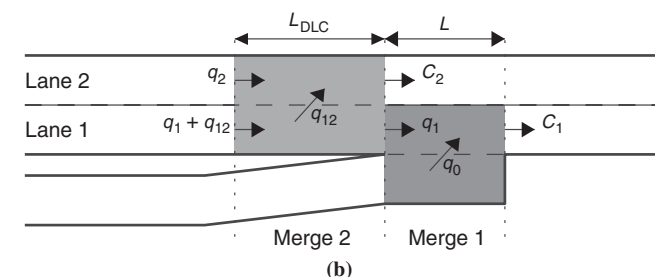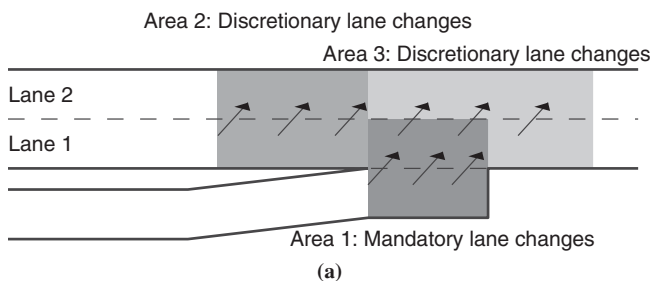$$\alpha_l = \frac{q_0}{q_1} \quad \text{(Merge 1)} \tag{2}$$

FIGURE 1   Sketch of a multilane merge: (a) lane-changing maneuvers and (b) spatial partitioning and notations.

Here, the definition for merge ratio α_l is not classical because the denominator does not correspond to the total inflow for all freeway lanes, as presented elsewhere (2, 3). The global merge ratio is denoted α_g when the total inflow is used as the denominator. In the modeling framework, α_g can simply be deduced from all system variables (flow values), that is, $\alpha_g = q_0/(q_1 + C_2)$ (Figure 1b). It would have been possible to directly use α_g to define the system of equations, but the authors decided to set the model parameters at the level of the local merges.

Analytical Expression of Effective Capacity for a Given Inserting Flow

The previous decomposition of a multilane merge into two non-overlapping local merges greatly simplifies the analytical investigations. Each merge has only one targeted lane for the insertions. The analytical expressions for the effective capacity, C_1 and C_2 for the related inserting flows q_0 and q_{12}, respectively, can then be derived directly from the analytical formulas provided elsewhere (24, 29). It is beyond the scope of this paper to explain how these formulas were derived. The authors recall only the main hypothesis and provide the formulation when vehicle characteristics are homogeneous. The readers are referred in particular to the work of Leclercq et al. for details and extension to the heterogeneous case (29).

Figure 2 presents how the analytical expression for the effective capacity can be derived by the use of Merge 1 as an example. Vehicle i inserts at time t_i at location x_i. Inserting positions are uniformly distributed over L, as shown previously for congested situations (30). The time lapse between two insertions (h_0) depends on the inserting flow; that is, h_0 is equal to $1/q_0$. Inserting vehicles are considered moving bottlenecks on the targeted lane with initial speed v_0 and bounded acceleration a (25, 26). The behavior of platoons of vehicles upstream of each moving bottleneck (shaded area in Figure 2) is described by the kinematic wave theory and a triangular fundamental diagram with wave speed w and jam density κ (27, 28). Free-flow speed has no influence because the focus is only on congested traffic states.

Each inserting vehicle generates a traffic wave that propagates backward at speed w until it reaches the origin of the on-ramp; that is, x is equal to 0 at time t'. Such a wave can reach x equal to 0 without perturbations (for example, Vehicle 1 in Figure 2) but can also meet a void downstream of an accelerating vehicle (for example, the wave from Vehicle 2 meets the void created by Vehicle 3 in Figure 2).

In the latter case, the wave is delayed until the void disappears and arrives later at x equal to 0. The mean capacity value can be calculated at any location because the flow is conserved. At x equal to 0, it appears that the flow evolution is composed of repetitive patterns that start again every time that a wave crosses x equal to 0. The tenets of the variational theory make it possible to derive the long-term mean capacity value C_1 by calculation of the mean flow values separately for each pattern (31):

$$C_1 = \frac{w\kappa}{h_0}\left(h_0 - T(h_0) + \frac{1}{2}s^2\frac{aw^2}{\gamma^3(h_0)} - \frac{1}{2}c^2\frac{2wh_0}{\gamma^3(h_0)}\right) \quad (3)$$

where

$$T(h_0) = \frac{(-w - v_0 + \gamma(h_0))}{a}$$

$$\gamma(h_0) = \sqrt{(w + v_0)^2 + 2awh_0}$$

$$s^2 = \begin{cases} \dfrac{L^2}{6w^2} & \text{if } L \le wh_0 \\[2em] h_0^2\left(\dfrac{\left(L - \dfrac{wh_0}{\sqrt{6}}\right)}{\left(L + (\sqrt{6} - 2)wh_0\right)}\right)^2 & \text{if } L > wh_0 \end{cases}$$

$$c^2 = 2ap_{\text{int}}\left(T(h_0) - \frac{1}{2}s^2\frac{aw^2}{\gamma^3(h_0)}\right) + a\left(T^2(h_0) + \frac{1}{2}s^2\frac{2w^2(w + v_0)}{\gamma^3(h_0)}\right)$$

where p_{int} is the probability that a wave created by a vehicle will meet a void before reaching x equal to 0. Its analytical expression is provided by Equations 6 and 7 in a previously published paper (29). An extended formulation that considers heterogeneous vehicle characteristics was also provided previously (29). This consideration permits vehicle behaviors to be distributed and, in particular, allows cars and trucks with different mean jam densities (κ_c and κ_t, respectively) and mean acceleration capabilities (a_c and a_t, respectively) to be distinguished. In the latter case, the fraction of trucks is denoted p.
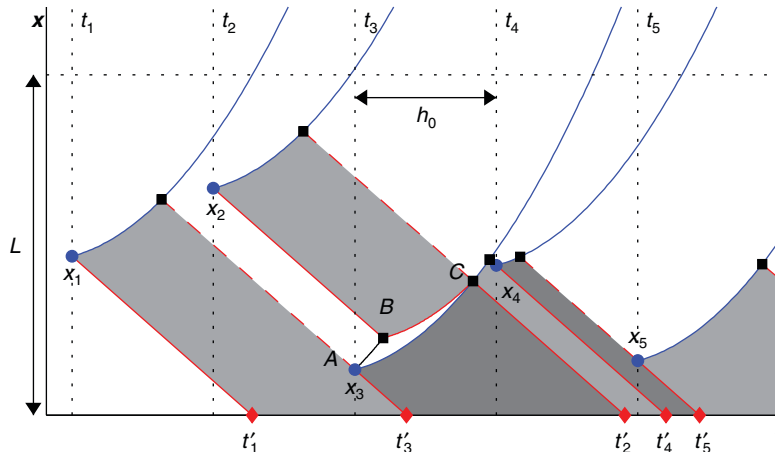

FIGURE 2 Derivation of analytical expression of effective capacity for the targeted lane.

Finally, it appears that C_1 and C_2 can be expressed as a function of q_0 and q_{12}, respectively. The initial speeds v_0 and v_1 for the inserting vehicles at Merges 1 and 2, respectively, are derived from the flow value observed on the origin lane by use of the fundamental diagram. Thus, Equation 1 can be refined and combined with Equation 2 to obtain

$$\begin{cases} q_0 + q_1 = C_1(q_0, v_0) \text{ with } v_0 = \dfrac{wq_0}{(w\kappa - q_0)} & \text{(Merge 1)} \\[2ex] q_1 = \dfrac{q_0}{\alpha_l} & \text{(Merge 1)} \\[2ex] q_{12} + q_2 = C_2(q_{12}, v_1) \text{ with } v_1 = \dfrac{w(q_1 + q_{12})}{(w\kappa - q_1 - q_{12})} & \text{(Merge 2)} \end{cases} \quad (4)$$

The system defined by Equation 4 has four unknowns, that is, q_0, q_{12}, q_1, and q_2, but only three equations. If the general expressions for the calculation of C_1 and C_2 provided previously are applied (*29*), the parameters involved are

- Wave speed (w),
- Truck fraction (p),
- Mean values for car and truck acceleration (a_c and a_t, respectively),
- Standard deviations for car and truck acceleration ($s_{a,c}$ and $s_{a,t}$, respectively),
- Mean values for car and truck jam densities (κ_c and κ_t, respectively), and
- Standard deviations for car and truck jam densities ($s_{\kappa,c}$ and $s_{\kappa,t}$, respectively).

Analytical Expression for Discretionary Lane Changes and Merge 2

A fourth equation can be added to the previous system by use of a focus on the lane-changing flow of Merge 2. A simple but continuous lane-changing model for discretionary maneuvers was described previously (*32*). The analytic expression of the macroscopic lane-changing rate (Φ) per unit of space is given by

$$\Phi(k_i, k_j) = \min\left(1, \frac{\mu(k_j)}{\lambda(k_j)}\right) \lambda(k_i) \frac{\max(v_j - v_i, 0)}{u^2 \tau} \quad (5)$$

where

k_i and k_j = densities on the origin and the targeted lanes, respectively;
v_i and v_j = speeds on the origin and the targeted lanes, respectively;
λ = demand function, that is, $\lambda(k) = \min(uk, uw\kappa/(w + \kappa))$;
μ = supply function, that is, $\mu(k) = \min(uw\kappa/(w+\kappa), w(\kappa - k))$;
u = free-flow speed; and
τ = a parameter that represents the duration of a lane-changing maneuver.

Here the focus is on situations in which both Lanes 1 and 2 are congested. Both demand functions then reduce to the maximal capacity. The supply on Lane 2 can be approximated by the outflow, that is, C_2. Thus, Equation 5 becomes

$$\Phi(k_i, k_j) = C_2 \frac{\max(v_2 - v_1, 0)}{u^2 \tau} \quad (6)$$

Finally, the lane-changing flow q_{12} can be determined by integration of Φ over the spatial extend of Merge 2. It comes that

$$q_{12} = C_2 \frac{\max(v_2 - v_1, 0)}{u^2 \tau} L_{\text{DLC}} \quad (7)$$

Speed v_2 can be derived from the flow on Lane 2 by use of the fundamental diagram. In the end, the authors were able to define a system of four equations and four unknowns for a merge with two lanes on the freeway and one lane on the on-ramp (see Equation 8). The numerical solutions can easily be computed by use of a classical solver like the classical solvers presented elsewhere (*24, 33*). The total effective capacity C is equal to $C_1 + C_2$ but also to $q_0 + q_1 + q_{12} + q_2$.

$$\begin{cases} q_0 + q_1 = C_1(q_0, v_0) \text{ with } v_0 = \dfrac{wq_0}{(w\kappa - q_0)} & \text{(Merge 1)} \\[2ex] q_1 = \dfrac{q_0}{\alpha_l} & \text{(Merge 1)} \\[2ex] q_{12} + q_2 = C_2(q_{12}, v_1) \text{ with } v_1 = \dfrac{w(q_1 + q_{12})}{(w\kappa - q_1 - q_{12})} & \text{(Merge 2)} \\[2ex] q_{12} = C_2 \dfrac{\max(v_2 - v_1, 0)}{u^2 \tau} L_{\text{DLC}} \text{ with } v_2 = \dfrac{wq_2}{(w\kappa - q_2)} & \text{(Merge 2)} \end{cases}$$
$$(8)$$

NUMERICAL INVESTIGATIONS

In this section, a sensitivity analysis is first performed to identify the parameters that are the most influential on the effective capacity per lane and the total effective capacity. The results obtained with the analytical model are then compared with the numerical results provided by a microscopic traffic simulator. Such a simulator provides a refined description of lane-changing maneuvers and the related traffic dynamics. This procedure permits testing of the relevance of the analytical model as a first approximation for the effective capacity values.

Local Sensitivity Analysis

In the reference scenario, the two-lane freeway has the following parameters: $L = 150$ m, $L_{\text{DLC}} = 100$ m, $\alpha_l = 1$, $\tau = 1.3$ s, $p = 15\%$, $a_c = 2$ m/s^2, $a_t = 1$ m/s^2, $s_{a,c} = 0$ m/s^2, $s_{a,t} = 0$ m/s^2, $\kappa_c = 0.145$ vehicles per meter (vpm), $\kappa_t = 0.067$ vpm, $s_{\kappa,c} = 0$ vpm, $s_{\kappa,t} = 0$ vpm, $w = 5.38$ m/s, and $u = 31.9$ m/s. Figure 3 presents the results of the sensitivity analysis for the first seven parameters. The parameters from the reference scenario were independently tested. Combined effects were thus not studied here.

In all cases, C_1 appeared to be lower than C_2. This finding corresponds to the expectation because the capacity restriction for low-speed vehicle insertions is supposed to be maximal close to the on-ramp. Figure 3*a* shows that the length of the on-ramp influences the effective capacity on Lane 1 only when L is less than 150 m. C_1 is reduced from 0.39 to 0.35 vehicles per second (vps) (-10%) when L is cut from 150 to 50 m. L has no influence on C_2. This finding is not surprising when the modeling framework proposed here is considered because inserting vehicles from the on-ramp are not allowed to change lanes again. On the contrary, the length of the discretionary lane-changing area influences C_2 only (Figure 3*b*).
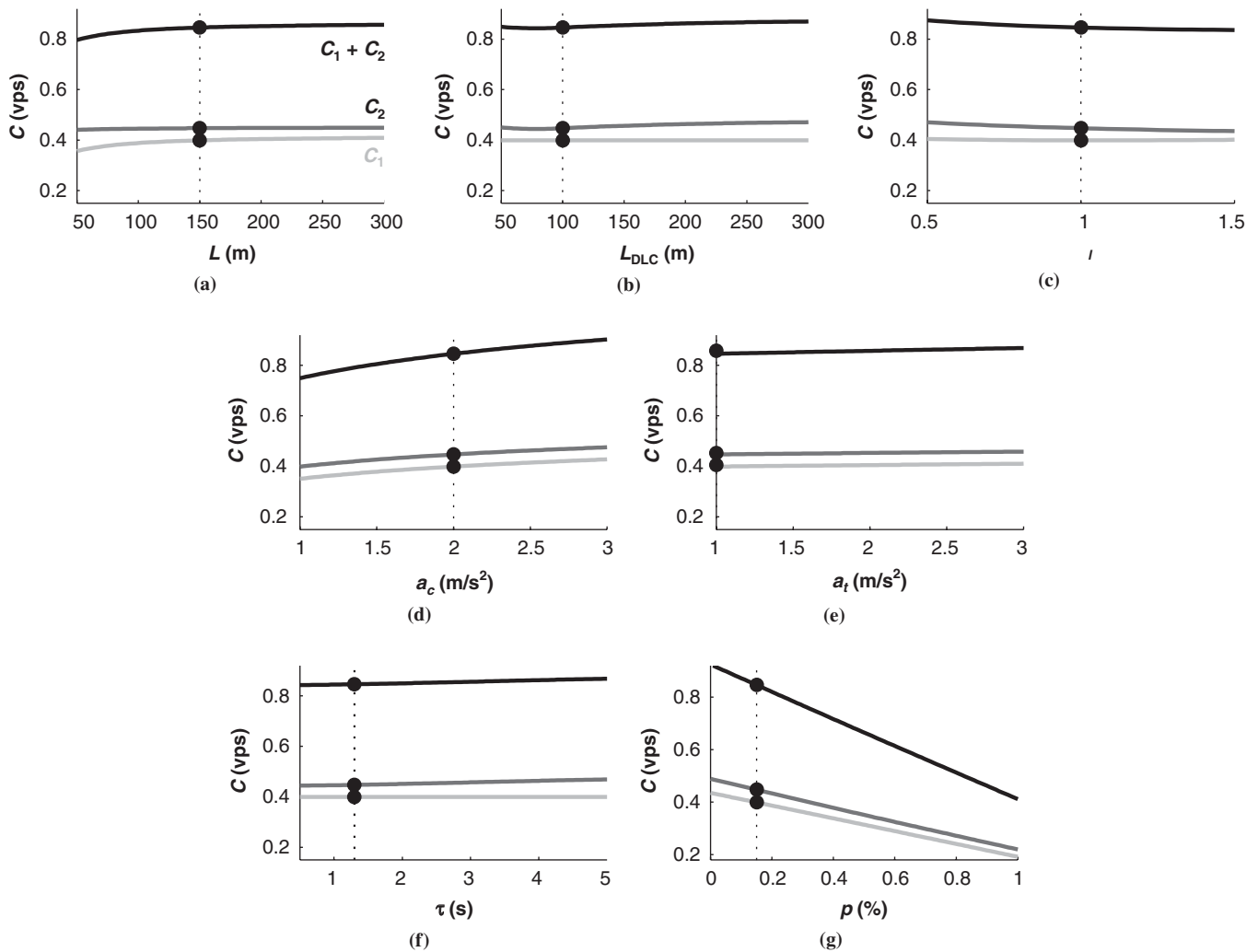
FIGURE 3   Sensitivity analysis by parameter: (a) length of the on-ramp (L), (b) length of the discretionary lane-changing area (L_{DLC}), (c) local merge ratio (α_l), (d) car acceleration (a_c), (e) truck acceleration (a_t), (f) time to complete a lane-changing maneuver (τ), and (g) fraction of trucks (p).

The variations are quite small, with no more than a 6% difference between the lowest C_2 value when L_{DLC} is equal to 80 m and the highest C_2 value when L_{DLC} is equal to 300 m being seen. C_2 slightly increases when L_{DLC} increases. This finding should be the result of the combination of two effects: the lane-changing flow should increase because more space is available for the lane-changing maneuvers but the initial speed should be higher, which limits the impact of inserting vehicles on Lane 2.

Figure 3c confirms an important result already highlighted elsewhere (24): the local merge ratio has almost no influence on C_1. A higher merge ratio means a higher inserting flow and so a higher speed on the on-ramp, whereas a lower merge ratio means a lower inserting flow but also a lower speed. In the latter case, few insertions are observed, but they individually create a stronger capacity reduction. The finding that both effects compensate for the local merge ratio when the local merge ratio changes is remarkable. The analysis can be taken further by study of the effect on Lane 2. C_2 is higher for the lowest α_l values. The C_2 value varies from 0.47 to 0.43 vps when α_l increases from 0.5 to 1.5. Lower α_l values mean a lower inserting flow and a higher flow upstream of the on-ramp in Lane 1. Thus, the

initial speed for discretionary lane changes is higher, which should reduce the influence of lane-changing maneuvers on lane 2.

Figure 3d shows that car acceleration significantly influences C_1 and C_2. The C_1 value increases from 0.35 to 0.41 vps (+17%) and C_2 increases from 0.4 to 0.46 vps (+15%) when a_c increases from 1 to 2.5 m/s². The acceleration has previously been proven to be the parameter that is most influential on the effective capacity (24, 29). This finding was confirmed here in a multilane context. Figure 3e shows the influence of truck acceleration. This influence looks to be limited, but this is because the truck fraction is low, only 15%. Thus, few trucks, on average, change lanes.

Figure 3e presents the influence of the duration of the discretionary lane-changing maneuvers. The duration of the discretionary lane-changing maneuvers has no influence on C_1 because lane changes are mandatory for Merge 1. The C_2 value increases from 0.44 to 0.46 vps (+5%) when τ increases from 1 to 4. Higher τ values mean that lane changes from Lane 1 to Lane 2 are harder, and this difficulty leads to a less severe capacity reduction on Lane 2. Finally, Figure 3f shows the influence of the fraction of trucks. As expected, the effective capacities on both lanes are very sensitive to this parameter.

Comparison with a Multilane Traffic Simulator

The multilane analytical model entails an aggregate description of the impacts of lane changing. Furthermore, it neglects the relaxation effect that usually happens after vehicle insertion in the target lane (*32, 34*). Vehicles tend to accept gaps shorter than the equilibrium (safe) one when they change lanes and then progressively adapt their spacing with their leader. To test the relevance of the analytical formulas, the effective capacity per lane was compared with the results provided by numerical simulations. Here, a microscopic traffic simulation based on Newell's model was used (*35*). This model is fully consistent with the kinematic wave theory when the fundamental diagram is triangular (*31*).

Discretionary lane-changing rules correspond to the discrete formulation of the continuum model defined by Equation 5. Details are provided elsewhere (*32*). A relaxation process is included after vehicle insertion. A constant speed difference equal to ε is maintained between a follower and its leader until the equilibrium spacing, defined by the fundamental diagram, is reached. Details about this are also provided elsewhere (*32*). Mandatory lane changes are governed by Daganzo's model (*2*) (also see Equation 2). In practice, the insertion rate is set to maintain on average a fixed local merge ratio between the on-ramp and the right lane. To ensure consistency between the numerical and the analytical results, discretionary lane changes were not allowed downstream of the on-ramp. Additional tests that relaxed this assumption were performed in the numerical simulator, and few differences in the effective capacity values were found.

Figure 4 compares the numerical results (dots) and the analytical results (lines) for the reference scenario but with a single class of vehicles with a mean acceleration equal to 1.2 m/s². The relaxation parameter ε was set to a classical value, that is, 1.62 m/s (*32*). Red plots correspond to the effective capacity for Lane 1, whereas blue plots are for Lane 2. Different values of τ, the parameter for the discretionary lane-changing process, were tested, and the results are shown in Figure 4*a*. A test that focused on the parameter that most influences the capacity drop, that is, acceleration (*a*), was performed, and the results are shown in Figure 4*b*.

Both Figure 4*a* and Figure 4*b* highlight that the analytical formulas provide good estimates of the effective capacity per lane in comparison with the numerical results. The results are very close for all values of τ. The results are also close for a wide range of acceleration values, that is, acceleration values of between 0.8 and 1.8 m/s². Some

discrepancies appeared for very low or very high acceleration rates. A possible explanation is that the relaxation process induced lower speeds for followers that locally reinforce the capacity restrictions compared with those obtained by strict application of the moving bottleneck theory. Another possible explanation is that insertions in the simulation are not necessarily uniformly distributed in space and time.

The blue and red bands in Figure 4*b* correspond to the numerical simulations performed with lower ε values (the upper bound of the band) and higher ε values (lower bound of the band), respectively. ε varied from 0.75 to 2.5 m/s². This finding confirms the authors' expectation that low acceleration values, which reduce the speed difference between inserting vehicles and their leaders, lead to effective capacity values closer to the analytical estimate. A remarkable result is that whatever acceleration value was used, the analytical estimate always fell within the band that corresponds to feasible ε values. The same result is observed in Figure 4*a*.

A traffic simulation with behavioral rules that are close to the behavioral assumptions of the analytical model was chosen because the purpose was to test if the analytical model reproduces local vehicle interactions resulting from traffic dynamics well enough compared with those obtained in a situation in which all interactions are directly and properly considered. This test appears to be conclusive. The authors did not try to compare the analytical model with a more complex traffic simulation and, notably, a commercial one because, to the best of the authors' knowledge, none has been proved to reproduce the capacity drop phenomenon accurately. For a more global proof, the authors prefer to resort to experimental observations, as shown in the next section.

FIRST EXPERIMENTAL VALIDATION

The experimental validation was performed for a merge located on a southbound three-lane segment of the M6 Motorway near Manchester, United Kingdom (geographical coordinates, 53°25′ 14.85″N, 2°34′42.18″E). Figure 5*a* presents a sketch of the merge. Because this freeway is in the United Kingdom, vehicles drive on the left. A loop detector (Loop Detector M7072) was located 1,600 m downstream of the merge. Two loop detectors were located just upstream (Loop Detector M7092) and downstream (Loop Detector M7088) of the merge. They provide flow and speed observations for each lane every minute.
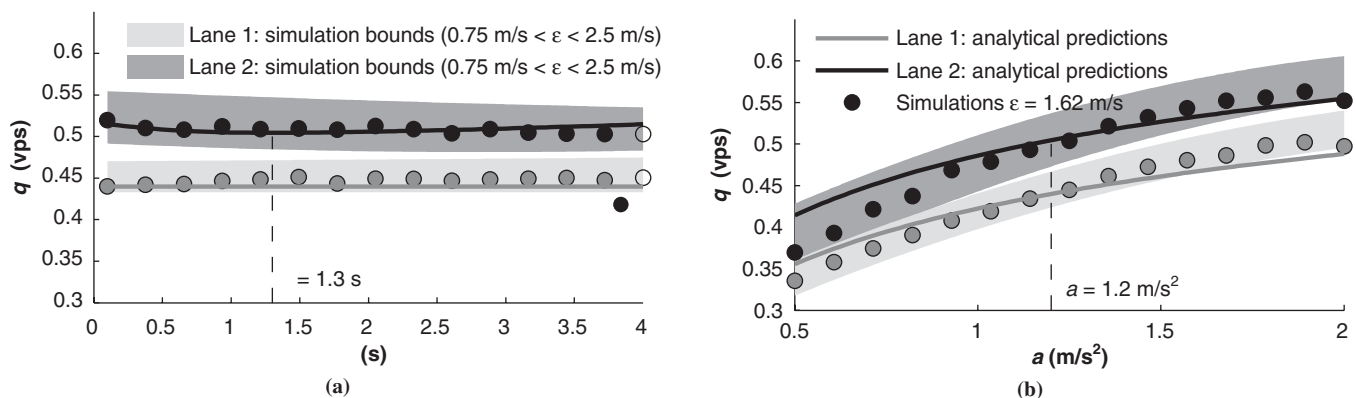

FIGURE 4 Comparison with simulation results: (*a*) effective capacities for Lanes 1 and 2 with respect to τ and (*b*) effective capacities for Lanes 1 and 2 with respect to *a*.
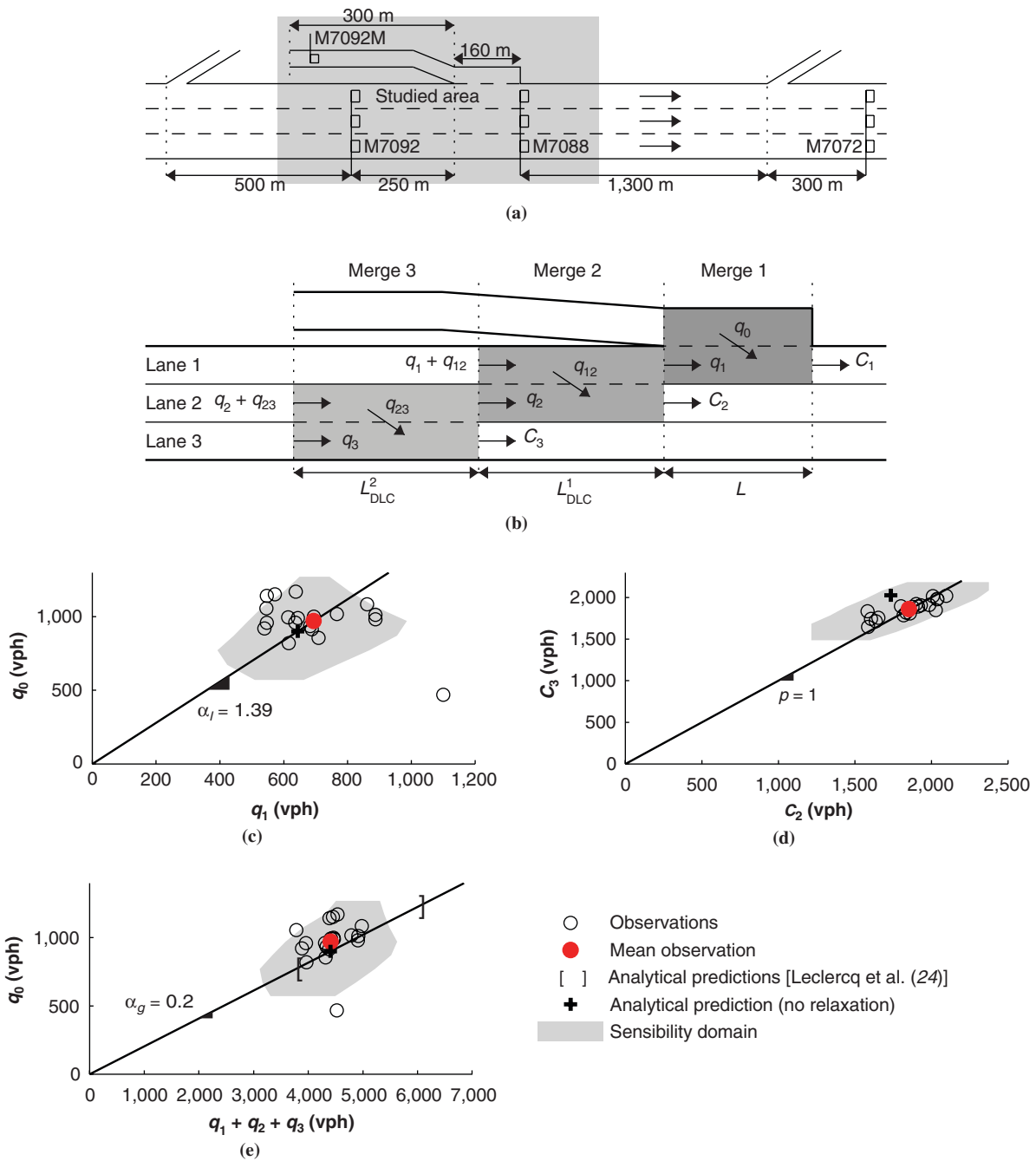
FIGURE 5 Experimental validation: (a) sketch of the experimental site, (b) partitioning of lane-changing maneuvers for a three-lane freeway, (c) inserting flow versus right-lane flow, (d) center versus left-lane effective capacity, and (e) inserting flow versus total effective capacity (vph = vehicles per hour).

Inserting flows were calculated on the basis of the difference of the total flow at these two stations with a 1-min lag. This lag roughly represents the time that a vehicle needs to travel from Loop Detector M7092 to Loop Detector M7088 in congestion. All data from May 2006 were available. Data from 6 business days when congestion was observed at the merge during the morning or the peak hours were selected, and data on free-flow conditions were obtained at Loop Detector M7072. This information guarantees that the merge is active (head of the queue). The focus here was only on heavy congestion, in which the speeds at Loop Detectors M7088 and M7092 were less than 50 km/h for all lanes. Finally, data collected over 1 min were aggregated over 20-min periods because the primary interest here was to study the mean effective capacity value per lane. In the end, 17 sets of observations were available for Loop Detectors M7092 and M7088, corresponding to data for 20 min of heavy congestion.

To perform the validation, the modeling framework first needed to be extended to account for three lanes on the freeway. Figure 5b shows how this can be implemented in a straightforward manner. A third merge was introduced between Lane 2 and Lane 3 upstream

of the first two merges. This third merge accounts for the discretionary lane changes from Lane 2 to Lane 3 and fulfills the condition of non-overlap with the other local merges. In reality, lane changes from Lane 2 to Lane 3 can also happen downstream, but the point here is that it is the region where lane changes occur that has the most impact on the capacity of Lane 3 for congested situations.

The lengths of the lane-changing areas for Merges 2 and 3 are denoted L_{DLC}^1 and L_{DLC}^2, respectively. The third merge comes with two new unknowns, which are the lateral flow between Lanes 2 and 3 (q_{23}) and the upstream flow on Lane 3 (q_3), and two equations, one of which is similar to Equation 7, which describes the exchange of flow between Lanes 2 and 3, and one of which is similar to Equation 3, which provides the effective capacity formulation C_3 for Lane 3.

A well-defined system with six equations and six unknowns was obtained, and a numerical solver was used to obtain the solution. Observations for each lane at Loop Detector M7088 were directly used to determine the values of C_1, C_2, and C_3 because this loop detector is just downstream of the merge. To estimate the values of q_1, q_2, and q_3, that analysis started with the upstream observations Q_1, Q_2, and Q_3 provided by Loop Detector M7092. Under the assumption that lane-changing maneuvers were only from the left to the right (from Lane 1 to Lane 2 or from Lane 2 to Lane 3), the following were determined: $q_3 = Q_3$, $q_2 = Q_2 - C_3 + q_3$, $q_1 = Q_1 - C_2 + q_2$.

The triangular fundamental diagram for this experimental site has been calibrated with the following values: $w = 19.4$ km/h, $u = 115$ km/h, and $\kappa = 145$ vehicle kilometers per lane (*36*). The truck ratio (p) was set equal to 0. The maximal acceleration and the discretionary lane-changing duration were set to typical values without further calibration: $a = 1.8$ m/s² and $\tau_1 = \tau_2 = 3$ s. The length of the on-ramp (L) was 160 m. The lengths of both discretionary lane-changing areas (L_{DLC}^1 and L_{DLC}^2) were set equal to 100 m. This parameter has been shown to have few impacts on the effective capacities by sensitivity analysis. Figure 5*c* shows the experimental results for q_0 versus q_1. Empty circles correspond to the 17 time periods, whereas the red circle is the average for all periods. The last observation was used to calibrate the local merge ratio, that is, α_l, which was equal to 1.39. Figure 5*d* presents the experimental results for C_2 versus C_3. A noticeable point here is that the experimental distribution was uniform for all congested periods, that is, $C_2 \approx C_3$.

Figure 5*e* presents the result for the global validation, that is, the relation between the on-ramp and the total upstream flows. It appears that the analytical model (green cross in Figure 5*e*) provides a very close estimate of the total capacity, that is, 5,305 vehicles per hour (vph) (−1.4%) compared with a total capacity of 5,380 vph for the average of the experimental observations (red circle). Furthermore, the global merge ratio (α_g) that resulted from the lane flow distribution predicted by the model was also very close to the real one: 0.22 and 0.2, respectively. This result is remarkable because, as mentioned in the introduction, previous analytical work provided only very large upper and lower bounds for the total effective capacity in a multilane context (see the brackets in Figure 5*e*) (*24*). Figure 5, *c* and *d*, shows that the analytical model also predicts extremely well the values of the effective capacities per lane: $C_1 = 1,545$ vph, $C_2 = 1,735$ vph, and $C_3 = 2,026$ vph. The discrepancies obtained when the values of C_1, C_2, and C_3 from the analytical model were compared with the experimental values were equal to −7%, −6%, and +8.9%, respectively.

Finally, the blue-shaded areas in Figure 5, *c* to *e*, correspond to the results obtained with the analytical model when the parameters were varied within the following bounds: $0.5 \leq a \leq 2.5$ m/s², $50 \leq L_{DLC}^1 \leq$ 300 m, $50 \leq L_{DLC}^2 \leq 300$ m, $1 \leq \tau_1 \leq 5$ s, $1 \leq \tau_2 \leq 5$ s, and $1 \leq \alpha_l \leq 2$. Almost all the experimental observations for the different congestion periods fell within the areas with blue shading in Figure 5, *c* to *e*. This ends the demonstration of the performance of the analytical model for this experimental merge because the findings highlight that the analytical model can fit all individual observations with feasible parameter values.

CONCLUSION

This paper proposes an analytical framework to estimate the capacity drop when multilane freeway merges act as active bottlenecks. This framework provides first-order approximations of the mean effective capacity for all lanes. These estimates were shown to be consistent with the results obtained from a traffic simulator that fully describes vehicle interactions. It was also demonstrated at an experimental site that the estimates fit empirical observations made during heavy congestion very well, even though strong assumptions had to be made.

The formulation of the analytical model as a system of equations may look complex, but it provides an instantaneous solution when implemented as a script combined with a numerical solver. There is no need to replicate a huge number of simulation runs, such as with traffic simulators, or to analyze long-term on-field data time series to identify periods of congestion. This formulation can be used to design new merges or to refine real-time traffic estimation models by the use of updated capacity formulations for merges. The sensitivity analyses are straightforward, which helps to identify clearly the most influential factors and to shed light on how the different local phenomena and the different kinds of lane changes influence the effective capacity values per lane and in total.

Further studies are needed to validate the model with a large set of different experimental sites with different configurations (different numbers of lanes, different on-ramp lengths, and so forth). By use of the inputs provided previously, it will be easy to account for different truck ratios per lane and further refine the system (*29*). Finally, this paper provides the first analytical connection between the local and the global merge ratios. Such a connection was previously investigated from an experimental perspective with a focus on the lane flow distribution (*6*). Here the macroscopic lane flow distribution was an output of the analytical model and resulted from a process of averaging of local phenomena. Use of this procedure may help to provide a better understanding of traffic behavior at merges and improve control algorithms.

REFERENCES

1. Newell, G.F. *Applications of Queueing Theory,* 2nd ed. Chapman & Hall, New York, 1982.
2. Daganzo, C. The Cell Transmission Model. Part II. Network Traffic. *Transportation Research Part B,* Vol. 29, No. 2, 1995, pp. 79–93.

3. Bar-Gera, H., and S. Ahn. Empirical Macroscopic Evaluation of Freeway Merge-Ratios. *Transportation Research Part C,* Vol. 18, 2010, pp. 457–470.

4. Troutbeck, R. J. The Performance of Uncontrolled Merges Using a Limited Priority Process. In *Proceedings of the 15th International Symposium on Transportation and Traffic Theory* (M. A. P. Taylor, ed.), Pergamon, Amsterdam, Netherlands, 2002, pp. 463–482.

5. Cassidy, M. J., and S. Ahn. Driver Turn-Taking Behavior in Congested Freeway Merges. In *Transportation Research Record: Journal of the Transportation Research Board, No. 1934,* Transportation Research Board of the National Academies, Washington, D.C., 2005, pp. 140–147.

6. Reina, P., and S. Ahn. Prediction of Merge Ratio Using Lane Flow Distribution. Presented at 93rd Annual Meeting of the Transportation Research Board, Washington, D.C., 2014.

7. Yuan, K., V. L. Knoop, and S. Hoogendoorn. Capacity Drop: Relationship Between Speed in Congestion and the Queue Discharge Rate. In *Transportation Research Record: Journal of the Transportation Research Record, No. 2491,* Transportation Research Board, Washington, D.C., 2015, pp. 72–80.

8. Cassidy, M. J., and R. L. Bertini. Some Traffic Features at Freeway Bottlenecks. *Transportation Research Part B,* Vol. 33, No. 1, 1999, pp. 25–42.

9. Hall, F. L., and K. Agyemang-Duah. Freeway Capacity Drop and the Definition of Capacity. In *Transportation Research Record 1320,* TRB, National Research Council, Washington, D.C., 1991, pp. 91–98.

10. Elefteriadou, L., R. P. Roess, and W. R. McShane. Probabilistic Nature of Breakdown at Freeway Merge Junctions. In *Transportation Research Record 1484,* TRB, National Research Council, Washington, D.C., 1995, pp. 80–89.

11. Persaud, B., S. Yagar, and R. Brownlee. Exploration of the Breakdown Phenomenon in Freeway Traffic. In *Transportation Research Record 1634,* TRB, National Research Council, Washington, D.C., 1998, pp. 64–69.

12. Chung, K., J. Rudjanakanoknad, and M. J. Cassidy. Relation Between Traffic Density and Capacity Drop at Three Freeway Bottlenecks. *Transportation Research Part B,* Vol. 41, No. 1, 2007, pp. 82–95.

13. Sarvi, M., M. Kuwahara, and A. Ceder. Observing Freeway Ramp Merging Phenomena in Congested Traffic. *Journal of Advanced Transportation,* Vol. 41, No. 2, 2007, pp. 145–170.

14. Oh, S., and H. Yeo. Estimation of Capacity Drop in Highway Merging Sections. In *Transportation Research Record: Journal of the Transportation Research Board, No. 2286,* Transportation Research Board of the National Academies, Washington, D.C., 2012, pp. 111–121.

15. Srivastava, A., and N. Geroliminis. Empirical Observations of Capacity Drop in Freeway Merges with Ramp Control and Integration in a First-Order Model. *Transportation Research Part C,* Vol. 30, 2013, pp. 161–177.

16. Cassidy, M. J., and J. Rudjanakanoknad. Increasing Capacity of an Isolated Merge by Metering Its On-Ramp. *Transportation Research Part B,* Vol. 39, No. 10, 2005, pp. 896–913.

17. Laval, J. A., M. J. Cassidy, and C. F. Daganzo. Impacts of Lane Changes at On-Ramp Bottlenecks: A Theory and Strategies to Maximize Capacity. In *Traffic and Granular Flow '05'* (R. Kühne, T. Poeschl, A. Schadschneider, M. Schreckenberg, and D. Wolf, eds.), Springer, Berlin, 2005, pp. 577–586.

18. Treiber, M., A. Kesting, and D. Helbing. Understanding Widely Scattered Traffic Flows, the Capacity Drop, and Platoons as Effects of Variance-Driven Time Gaps. *Physical Review E,* Vol. 74, No. 2, 2006, pp. 1–10.

19. Laval, J. A., and C. F. Daganzo. Lane-Changing in Traffic Streams. *Transportation Research Part B,* Vol. 40, No. 3, 2006, pp. 251–264.

20. Coifman, B., and S. Kim. Extended Bottlenecks, the Fundamental Relationship and Capacity Drop. *Transportation Research Part A,* Vol. 45, No. 9, 2011, pp. 980–991.

21. Chen, D., S. Ahn, J. A. Laval, and Z. Zheng. On the Periodicity of Traffic Oscillations and Capacity Drop: The Role of Driver Characteristics. *Transportation Research Part B,* Vol. 59, 2014, pp. 117–136.

22. Carlson, R. C., I. Papamichail, and M. Papageorgiou. Integrated Feedback Ramp Metering and Mainstream Traffic Flow Control on Motorways Using Variable Speed Limits. *Transportation Research Part C,* Vol. 46, 2014, pp. 209–221.

23. Kim, S., and B. Coifman. Driver Relaxation Impacts on Bottleneck Activation, Capacity, and the Fundamental Relationship. *Transportation Research Part C,* Vol. 36, 2013, pp. 564–580.

24. Leclercq, L., J. A. Laval, and N. Chiabaut. Capacity Drops at Merges: An Endogenous Model. *Transportation Research Part B,* Vol. 45, No. 9, 2011, pp. 1302–1313.

25. Newell, G. F. A Moving Bottleneck. *Transportation Research Part B,* Vol. 32, No. 8, 1998, pp. 531–537.

26. Leclercq, L., S. Chanut, and J.-B. Lesort. Moving Bottlenecks in Lighthill–Whitham–Richards Model: A Unified Theory. In *Transportation Research Record: Journal of the Transportation Research Board, No. 1883,* Transportation Research Board of the National Academies, Washington, D.C., 2004, pp. 3–13.

27. Lighthill, M. J., and J. B. Whitham. On Kinematic Waves. II. A Theory of Traffic Flow in Long Crowded Roads. *Proceedings of the Royal Society of London A: Mathematical, Physical and Engineering Sciences,* Vol. 229, No. 1178, 1955, pp. 317–345.

28. Richards, P. I. Shockwaves on the Highway. *Operations Research,* Vol. 4, 1956, pp. 42–51.

29. Leclercq, L., V. L. Knoop, F. Marczak, and S. P. Hoogendoorn. Capacity Drops at Merges: New Analytical Investigations. *Transportation Research Part C,* Vol. 62, 2016, pp. 171–181.

30. Daamen, W., M. Loot, and S. P. Hoogendoorn. Empirical Analysis of Merging Behavior at Freeway On-Ramp. In *Transportation Research Record: Journal of the Transportation Research Board, No. 2188,* Transportation Research Board of the National Academies, Washington, D.C., 2010, pp. 108–118.

31. Daganzo, C. F. A Variational Formulation of Kinematic Waves: Basic Theory and Complex Boundary Conditions. *Transportation Research Part B,* Vol. 39, No. 2, 2005, pp. 187–196.

32. Laval, J. A., and L. Leclercq. Microscopic Modeling of the Relaxation Phenomenon Using a Macroscopic Lane-Changing Model. *Transportation Research Part B,* Vol. 42, No. 6, 2008, pp. 511–522.

33. Marczak, F., L. Leclercq, and C. Buisson. A Macroscopic Model for Freeway Weaving Sections. *Computer-Aided Civil and Infrastructure Engineering,* Vol. 30, No. 6, 2015, pp. 464–477.

34. Hidas, P. Modelling Vehicle Interactions in Microscopic Simulation of Merging and Weaving. *Transportation Research Part C,* Vol. 13, 2015, pp. 37–62.

35. Newell, G. F. A Simplified Car-Following Theory: A Lower Order Model. *Transportation Research Part B,* Vol. 36, No. 3, 2002, pp. 195–205.

36. Chiabaut, N., L. Leclercq, T. Bretin, and C. Buisson. Calibrating the Fundamental Diagram in Congestion: Methods Based on Observations at Consecutive Loop-Detectors. In *Proceedings of the IWTDCS Conference,* Barcelona, Spain, University of Tokyo, 2008.